Polyelectrolyte Titration: Theory and Experiment

Itamar Borukhov,*,† David Andelman,‡,|| Regis Borrega,† Michel Cloitre,† Ludwik Leibler,† and Henri Orland§,⊥

Unité Mixte de Recherche CNRS/ATOFINA (UMR 167), 95 rue Danton, B.P. 108, 92303 Levallois-Perret Cedex, France, School of Physics and Astronomy, Raymond and Beverly Sackler Faculty of Exact Sciences, Tel Aviv University, Tel Aviv 69978, Israel, and Service de Physique Théorique, CE-Saclay, 91191 Gif-sur-Yvette Cedex, France

Received: May 23, 2000; In Final Form: July 31, 2000

Titration of methacrylic acid/ethyl acrylate copolymers is studied experimentally and theoretically. At low salt concentrations, this polyacid exhibits a plateau in the titration curve below the neutralization point. The plateau has often been attributed to a first-order phase transition associated with polymer conformational changes. We argue that the specific shape of titration curves of hydrophobic polyelectrolytes is due to electrostatics and does not necessarily require a conformation change of the polyelectrolyte chains. We calculate the free energy at the mean-field level and its first-order (one loop) correction using a loop expansion. The latter is dominated by Debye−Hückel-like charge−charge correlations as well as by correlations between dissociation sites along the polymer chain. We show that the one-loop corrections to the free energy lead to titration curves that agree with experiments. In particular, the model explains the decrease of the pH at the plateau when the polymer concentration is increased or when salt is added to the solution.

I. Introduction

In recent years the search for environment-friendly materials has promoted the development of numerous water-soluble polymer applications. Polymers can be made water-soluble by making them compatible with the strong polar environment of the aqueous media, e.g., by introducing either charges or strong dipoles on the chains.[1−3]

Most charged polymers (polyelectrolytes) have a hydrophobic backbone. This hydrophobicity induces an effective attraction between monomers which competes with the Coulomb repulsion between charges. As a result, hydrophobic polyelectrolytes exhibit complex behavior including conformation changes, macro- and mesophase separation, self-association, and aggregation.[4−6]

Despite considerable theoretical and experimental effort, many questions remain open. In particular, the role of the coupling between hydrophobic attractions and long-range Coulomb interactions on the physicochemical properties of polyelectrolyte solutions is not fully understood. In this paper, we consider the role of such coupling in solutions of weak polyacids.

Weak acid monomers (denoted HA) can undergo dissociation of the type

$$HA \rightleftharpoons H^+ + A^-$$

where A^- is the charged monomer attached to the backbone, while the dissociated H^+ charge dissolves into the solution. The dissociation/association is an equilibrium process satisfying detailed balance. The ionization degree determines the effective amount of charge on the polyelectrolyte chain, and it depends on the pH of the solution. At low pH the polymer is weakly charged, whereas at high pH a larger fraction of monomers are dissociated and the polymer charge saturates to its maximal value. The most visible consequence is the solubility in water: hydrophobic polyacids can become water-soluble at high enough pH, where the polymer charge is strong enough to overcome the chain hydrophobicity. In contrast to low-molecular-weight acids, the charged groups of polyacids are correlated as they are linked together along the chain. Indeed, the dissociation of one acid group is correlated in a complex way to the position and number of other charged groups on the chain. As a result, when the amount of charge on the chain varies, the chain conformation is affected and in turn influences the dissociation of other groups.[4,5,7,8] Studies of the interplay of these competing effects have attracted a large amount of experimental[9−11] and theoretical[12−14] interest. Additional motivation for these efforts is related to the use of water-soluble polyelectrolytes, particularly alkali-swellable polymers, in many industrial applications, such as the coating, food, and cosmetic industries.[15,16]

An elementary and widespread experimental approach to characterizing polyacids is to perform titration experiments. In these experiments, a strong base such as NaOH is added to a solution of weakly charged polyelectrolytes. The pH of the solution and the equilibrium dissociation depend not only on the amount of added base (as for ordinary acids,[17]) but also on the polyelectrolyte concentration and the presence of salt.[18,19] The overall shape of the titration curve depends on the nature of the polyelectrolyte that is titrated.[18] In the case of poly(acrylic acid), the pH increases steadily with the dissociation degree. In contrast, the titration curve of poly(methacrylic acid) shows a maximum at low dissociation. Such a nonmonotonous dependence has been related to a conformational transition. The case of hydrophobic polyelectrolytes is still more intriguing: the

* Present address: Department of Chemistry and Biochemistry, University of California at Los Angeles, Los Angeles, CA 90095-1569. E-mail: itamar@chem.ucla.edu.
† Unité Mixte de Recherche CNRS/ATOFINA.
‡ Raymond and Beverly Sackler Faculty of Exact Sciences.
§ Service de Physique Théorique.
|| E-mail: andelman@post.tau.ac.il.
⊥ E-mail: orland@spht.saclay.cea.fr.

10.1021/jp001892s CCC: $19.00
Published on Web 10/25/2000

titration curve shows a large plateau where the pH is almost constant before the neutralization point is obtained. It has been argued in the literature that this plateau could be associated with a first-order phase transition between collapsed and swollen states of the polyacid chains.[8,20]

In this paper we show that this peculiar shape of the titration curves can be explained without relying on conformational phase transition of the polyacid chains. By including the effect of correlations of charges along the chains in the free energy, we calculate titration curves that show a behavior similar to the curves obtained in experiments. In particular, we explain how the pH depends on the polymer concentration and the amount of added salt. This dependence is special to polyacid solutions and is much weaker in monomeric acid solutions.

The paper is structured as follows: in the next section, the mean-field free energy, its one-loop correction, and the resulting titration equations and curves are presented. The experimental measurements of the titration of methacrylic acid/ethyl acrylate (MAA-EA) copolymers are discussed in section III, and the comparison between theory and experiment is presented in section IV. The full formalism relying on a field theoretical approach will be presented in a forthcoming publication.

II. Theory

We present first the free energy leading to titration curves of weak polyacids in the presence of added salt. Our system consists of four dissociating species: water, methacrylic acid monomers (denoted HA), NaOH titrating base, and NaCl salt. The dissociation reactions are written as:

$$H_2O \rightleftharpoons H^+ + OH^-$$

$$HA \rightleftharpoons H^+ + A^-$$

$$NaOH \rightarrow Na^+ + OH^-$$

$$NaCl \rightarrow Na^+ + Cl^-$$

The partial dissociation of water and acid monomers is accompanied by an energy cost associated with breaking the molecular bond. They are denoted as Δ_1 and Δ_2, respectively (in units of the thermal energy k_BT), and they are related to the mass action law,[17] as will be detailed below. Because NaOH is a strong base, it is fully dissociated. Similarly, the salt is fully dissociated.

The polymer used in the experiment is a statistical copolymer composed randomly of two monomers: methacrylic acid and ethyl acrylate. The total polymerization index is denoted as N. A fraction ($f = 1/3$) of the monomers are composed of the methacrylic acid, i.e., they are ionizable. Because the charged monomers are distributed uniformly along the chain, we assign a partial charge, fe, to each monomer ("smearing" the charges along the chain). Note that fe is the nominal charge of each monomer, whereas the actual charge is related to the partial dissociation of the acid monomers.

The concentration of monomers in the solution is denoted c_m, and the concentrations of the small ions are denoted c_H, c_{OH}, c_{Na}, and c_{Cl}.

The base concentration added to the solution is denoted c_B, and its ratio to the MAA monomer concentration is defined as the degree of neutralization γ:

$$\gamma \equiv \frac{c_B}{f c_m} \tag{1}$$

where γ varies between zero (no added base) and infinity (large base excess). It is also useful to define the degree of ionization, α, of the acid

$$\alpha = \frac{[A^-]}{[HA] + [A^-]} = \frac{[A^-]}{f c_m} \tag{2}$$

where $[A^-]$ and $[HA]$ are the concentrations of dissociated and nondissociated monomers, respectively. This degree of ionization is related to the $pH = -\log_{10} c_H$ of the solution via

$$pH = pK_a + \log_{10} \frac{\alpha}{1-\alpha} \tag{3}$$

In addition, because of charge neutrality, α and γ are related via

$$\alpha = \gamma + \frac{[H^-] - [OH^-]}{f c_m} \tag{4}$$

The conservation of mass implies the following relation between the ion concentrations:

$$c_{Na} = c_B + c_{Cl}$$

Note that the Cl^- ions come only from the salt, whereas the Na^+ ions come both from the base and the salt. Similarly, the OH^- ions come from the dissociation of water and base, whereas the H^+ ions come from the dissociation of water and monomeric acid.

A. Free Energy. We expand the full free energy in a loop expansion retaining the first two orders: $F = F_0 + \Delta F$, where F_0 is the mean-field term and ΔF is the one-loop correction. This expansion is valid provided that the concentrations of the various species present in the solution do not have strong fluctuations. This condition is satisfied in the experiments described below because the polymer concentration is above the overlap concentration (semidilute or concentrated regimes). As will be seen in sections III and IV, in the experiments the polymerization index is $N \simeq 10^4$, and the monomer size is $a \simeq 5$ Å. We estimate the overlap polymer concentration to be $c^* \simeq 10^{-6}$ Å^{-3} (1.6 mM). This estimate roughly agrees with that of viscosity measurements on dilute and semidilute solutions where $c^* \simeq 10^{-5}$ g/g (0.1 mM).[21] Because in the experiments the monomer concentrations c_m vary between 100 mM and 1 mM, corresponding to concentrations of roughly 6×10^{-4} to 6×10^{-6} Å^{-3}, we are always in the semidilute or concentrated regime, $c_m > c^*$. Below we discuss the two terms of the free energy separately.

1. Mean-Field Free Energy. In a separate work, the mean-field free energy (per unit volume and in units of k_BT) is shown to be

$$\begin{aligned}\beta F_0 = \frac{c_m}{N}(\log c_m\omega_m - 1) + \sum_{j=H,OH,Na,Cl} c_j (\log c_j\omega_j - 1) \\ - \frac{v}{2}c_m^{\,2} + \frac{w}{6}c_m^{\,3} - \lambda_0 c_m - (c_{OH} - c_B)\Delta_1 \\ - (c_H + c_B - c_{OH})\Delta_2 + (c_H + c_B - c_{OH})\,\beta e\varphi_0 \\ - f c_m \log(1 + e^{\beta e\varphi_0})\end{aligned} \tag{5}$$

This energy turns out to be identical to the usual Flory−Huggins free energy of polymer−solvent mixtures. The factor $1/N$ in the first term accounts for the reduction of translational entropy

of chains of N monomers. The second term represents the entropy of mixing of the small ions. The parameter ω_j is the molar volume of the j species. The next two terms represent the short-range monomer−monomer interactions. The hydrophobic effect is modeled by an attractive second virial coefficient υ (having the dimension of volume) and a repulsive third virial coefficient w (having a dimension equal to volume squared) introduced to avoid collapse of the chain. The next term represents the chain conformational entropy, where λ_0 is the conformational entropy per monomer of a free Gaussian chain.

The following two terms represent the energy cost of dissociation of water molecules and acid monomers. We define by Δ_1 the energy loss for each dissociation of a water molecule

$$H_2O \rightleftharpoons H^+ + OH^-$$

and by Δ_2 the energy loss for each dissociation of an acid molecule

$$HA \rightleftharpoons H^+ + A^-$$

The number of OH^- ions coming from dissociation of water molecules is equal to the difference between the total number of OH^- ions and those coming from the NaOH base. Similarly, the number of dissociated acid groups is equal to the difference between the total number of H^+ ions and the number of H^+ ions coming from the water.

Finally, the last two terms account for the electrostatic energy, φ_0 being the electrostatic potential in the solution. The first of these terms is the electrostatic energy of the small ions, and the second is the electrostatic free energy of partially dissociated monomers.[22]

2. One-Loop Correction to the Free Energy. The one-loop correction to the mean-field free energy ΔF will be presented in detail in a forthcoming publication. It is obtained by integrating over the quadratic fluctuations of the concentration fields. The correction term to the free energy is given (up to an additive constant) by

$$\beta\Delta F = \frac{1}{2}\int \frac{d^3\mathbf{q}}{(2\pi)^3}\log \Sigma(q) \tag{6}$$

$$\Sigma(q) = [1 + (wc_m - \upsilon)c_m N D(\eta)](q^2 + \kappa^2) + 4\pi l_B f^2 A^2 N D(\eta) c_m \tag{7}$$

$$\eta = \frac{1}{6}a^2 q^2 N \tag{8}$$

where the Debye−Hückel screening length, κ^{-1}, depends on the total concentration of small ions, c_I, and the effective charge of the chain, $fA(1 - A)c_m$:

$$\kappa^2 = 4\pi l_B(c_I + fA(1-A)c_m) \equiv 4\pi l_B c_{eff} \tag{9}$$

$$c_I = c_H + c_{OH} + c_B + 2c_{Cl} = c_H + c_{OH} + c_{Na} + c_{Cl} \tag{10}$$

The Bjerrum length is $l_B = e^2/\epsilon k_B T \simeq 7$Å. The dissociation fraction of the acid monomers is given by

$$A = \frac{e^{\beta e \varphi_0}}{1 + e^{\beta e \varphi_0}} \tag{11}$$

The Debye function[2] $D(\eta)$ entering eq 7 is given by

$$D(\eta) = \frac{2}{\eta}\left(1 + \frac{e^{-\eta} - 1}{\eta}\right) \tag{12}$$

In addition to the small ion contribution to the electrostatic screening, eq 9 includes a term proportional to $A(1 - A)$, where A is defined in eq 11 above. This term accounts for changes in the dissociation degree of monomers depending on the *local* electrostatic potential and represents the screening due to the dissociated monomers.[8,22] It is proportional to the charge density of dissociated monmers, i.e., $f Ac_m$. In addition, screening is due to mobile ions and to monomeric ions that can move (by association/dissociation) only along the chains and not in the entire volume of the solution. Therefore, in the above term there is also a factor $(1 - A)$ accounting for the fraction of available sites along the chain. For example, if all monomeric ions are dissociated, $A = 1$, the ions cannot move (by further dissociating) along the chain and do not contribute to the screening.

In our model, the concentrations c_{Na}, c_{Cl}, and c_m are fixed by the amount of NaCl salt, NaOH base, and polymer in the solution, whereas the concentrations of dissociated H^+ and OH^- ions depend on the degree of dissociation of water molecules and acid monomers (through the electrostatic potential, φ_0). Thus c_H, c_{OH}, and φ_0 are variational parameters, determined by the requirement that the free energy $F = F_0 + \Delta F$ be an extremum. In titration experiments c_H can be monitored directly through the pH of the solution.

3. Simplified Free Energy. To better understand the main contributions to the correction ΔF, let us return to the expression for $\Sigma(q)$, eq 7. First, we note that the Debye function is bound between 0 and 1 (see also eq 27). For typical values of the physical parameters (see also section IV)

$$\upsilon \simeq 25\text{Å}^3 \quad w \simeq 100\text{Å}^6$$
$$N \simeq 10^4 \quad c_m \simeq 1\ \text{mM} \tag{13}$$

it is easily seen that for long chains ($N \gg 1$), the Debye function can be approximated by $ND(\eta) \simeq 12/a^2q^2$, and

$$|wc_m - \upsilon| c_m N D(\eta) \ll 1 \tag{14}$$

Thus, the effect of the solvent quality is small and will be neglected in this section.

$$\Delta F \simeq \frac{1}{2}\int \frac{d^3\mathbf{q}}{(2\pi)^3}\log[q^2 + \kappa^2 + z] \tag{15}$$

where

$$z = 4\pi l_B f^2 A^2 N D(\eta) c_m \tag{16}$$

For the same range of parameters, eq 13, $\kappa^2 \gg z$, and ΔF can be expanded to first order in z, $\Delta F = \Delta F_0 + \Delta F_1$:

$$\Delta F_0 = \frac{1}{2}\int \frac{d^3\mathbf{q}}{(2\pi)^3}\log[q^2 + \kappa^2] \tag{17}$$

The integral can be calculated by including a cutoff at large q, which cancels out the Coulomb self-energy, yielding

$$\Delta F_0 = -\frac{\kappa^3}{12\pi} \tag{18}$$

This result is the well-known Debye−Hückel correlation energy of an electrolyte. The correction ΔF_1 is given by

$$\Delta F_1 \simeq \frac{1}{2}\int \frac{d^3\mathbf{q}}{(2\pi)^3}\frac{z}{q^2+\kappa^2} \simeq 6f^2A^2\frac{l_B\kappa^{-1}}{a^2}c_m \qquad (19)$$

This correction is due to correlations along the chain between dissociated monomers, as can be seen from the following simple argument. Consider the screened electrostatic interaction between charged monomers on a single infinite chain. For a specific chain configuration, the Coulomb energy per monomer is

$$U_{el} = \sum_{j\neq 0}\frac{f^2A^2e^2}{\epsilon|\mathbf{r}_j|}e^{-\kappa r_j} \qquad (20)$$

where r_j is the spatial distance between the $j = 0$ monomer and another $j = \pm 1, \pm 2, \ldots$ monomer. For an infinite Gaussian random walk, the typical (most probable) distance between monomers is given by

$$\langle r_j\rangle \simeq \left|\frac{2j}{3}\right|^{1/2} a \qquad j \gg 1 \qquad (21)$$

Assuming that r_j can be approximated by $\langle r_j\rangle$ in eq 20, and that $\kappa a \ll 1$, the sum over j can be replaced by a continuous integral leading to eq 19.

B. Titration Equations. The free energy depends on the species concentrations: c_{OH}, c_{Na}, c_H, c_m, and c_{Cl}. However, the concentration of monomers, Na^+ and Cl^- is fixed by the amount of polymer, base and salt added to the solution. On the other hand, the concentration of H^+ and OH^- ions is determined self-consistently by minimizing the full one-loop free energy $F = F_0 + \Delta F$, eqs 5 and 6, with respect to c_H, and c_{OH}, φ_0. The resulting equations of state determine the dependence of the pH of the solution on the other system parameters.

$$\log(c_H\omega_H) + \beta e\varphi_0 - \beta\Delta_2 + 2\pi l_B I_l = 0 \qquad (22)$$

$$\log(c_{OH}\omega_{OH}) - \beta e\varphi_0 - \beta\Delta_1 + \beta\Delta_2 + 2\pi l_B I_1 = 0 \qquad (23)$$

$$c_H + c_B - c_{OH} - fc_mA + 2\pi l_B f c_m A(1-A)[(1-2A)I_1 + 2ANfI_2] = 0 \qquad (24)$$

where the quantities I_1 and I_2 are defined as:

$$I_1 = \int_0^{\Lambda}\frac{k^2dk}{2\pi^2}\frac{1+Nc_m(wc_m-v)D(\eta)}{\Sigma(k)} \qquad (25)$$

$$I_2 = \int_0^{\Lambda}\frac{k^2dk}{2\pi^2}\frac{D(\eta)}{\Sigma(k)} \qquad (26)$$

and Λ is a short distance (large q) cutoff.

With the full expression (eq 12) of the Debye function $D(\eta)$, the integrals in eqs 25 and 26 cannot be performed analytically. However, for the values of the parameters used in the experiments, namely polymerization index $N \sim 10^4 - 10^5$ and monomer length $a \sim 5$ Å, it is possible to use a simplified form for the Debye function:

$$D(\eta) \simeq \frac{1}{1+\eta/2} \qquad (27)$$

As can easily be seen by comparing eq (27) with the exact expression (12), the above form has the right behavior both at small and large values of η. Within this approximation, the integrals are given by

$$I_1 = -\frac{1}{2\pi R^2}\frac{R^2\kappa^2\,\kappa_+\kappa_-/2 + (\lambda+1)\kappa^2 + u}{\kappa_+\kappa_-(\kappa_+ + \kappa_-)} \qquad (28)$$

$$I_2 = \frac{1}{2\pi R^2(\kappa_+ + \kappa_-)} \qquad (29)$$

where we have used the notation

$$\lambda = Nc_m(wc_m - v) \qquad (30)$$

$$u = 4\pi l_B A^2 N f^2 c_m \qquad (31)$$

$$R^2 = Na^2/6 \qquad (32)$$

and

$$\kappa_\pm^2 = \frac{1}{R^2}\left(\lambda + 1 + \frac{R^2}{2}\kappa^2 \pm \sqrt{(\lambda+1-R^2\kappa^2/2)^2 - 2uR^2}\right) \qquad (33)$$

Note that in eq 28 we have omitted a term, equal to $\Lambda/2\pi^2$, which exactly cancels the Coulomb self-energy.

Equations 22 and 23 can now be recast in the form

$$c_Hc_{OH} = 10^{-14}\,e^{-4\pi l_B I_1} \qquad (34)$$

which shows the change induced by fluctuations on the water dissociation constant and

$$c_H = \frac{1-A}{A}\,10^{-pK_a}\,e^{-2\pi l_B I_1} \qquad (35)$$

These two equations, together with eq 24, which expresses charge neutrality at the one-loop level, are solved iteratively. The numerical solution is obtained by using the mean-field values as a starting point for the iterations, and convergence is usually achieved after a few iterations.

C. Structure Function—*S*(*q*). In scattering experiments, the structure function $S(q)$ is readily obtained. It is related to the Fourier transform of the various density−density correlations in the sample. For example, we can regard the monomer−monomer correlations

$$S(q) = \langle\delta c_m(q)\delta c_m(-q)\rangle/c_m \qquad (36)$$

Because the one-loop expansion takes into account Gaussian fluctuations, it can also be used to calculate the structure function.[6,14,22] The result is

$$S^{-1}(q) = \frac{1}{ND(\eta)} + wc_m^2 - vc_m + \frac{f^2A^2 4\pi l_B c_m}{q^2+\kappa^2} \qquad (37)$$

The inverse structure function $S^{-1}(q)$ is the energy penalty associated with density fluctuations at a wavenumber q. A minimum in $S^{-1}(q)$ corresponds to the strongest fluctuating wavenumber q^*. As a result, incoming radiation at this wavenumber interacts most strongly with the sample, and a peak appears in the structure function (and, consequently, in the scattering intensity).

An instability appears when $S^{-1}(q)$ vanishes, corresponding to a divergence of the peak in the structure function. When the instability appears at a finite $q = q^*$ the system undergoes a

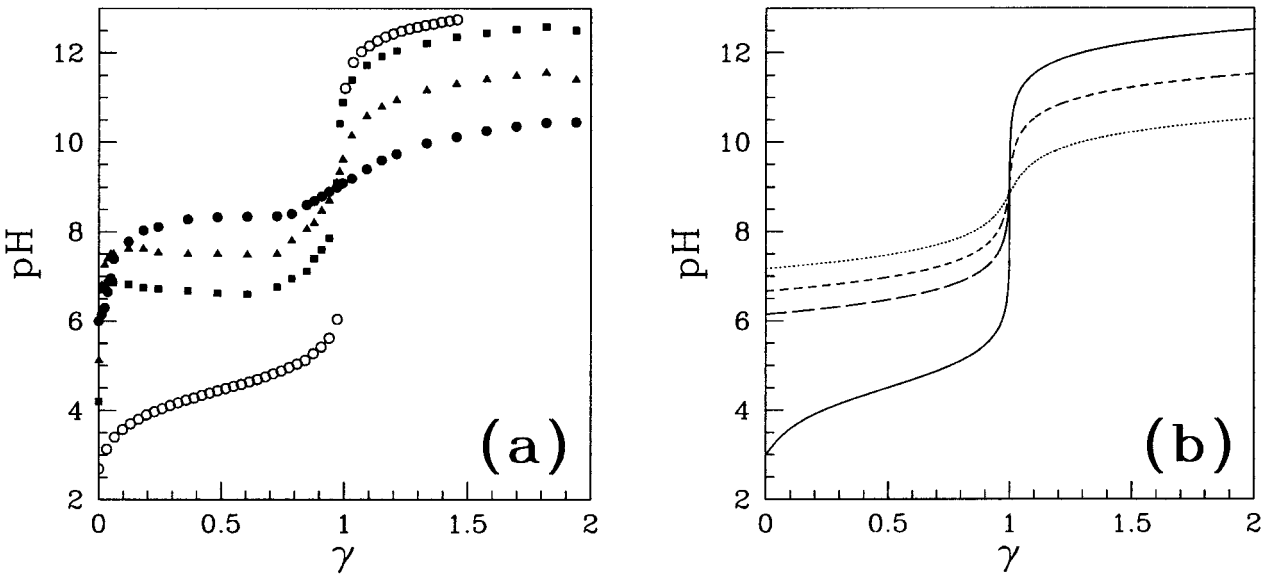

Figure 1. pH plotted as a function of the degree of neutralization γ with no added salt. In (a), the experimental titration curves are shown for different polymer concentrations: $c_m = 1$ mM (10^{-4} g/g), full circles; $c_m = 10$ mM (10^{-3} g/g), full triangles; $c_m = 100$ mM (10^{-2} g/g), full squares. The open circles denote the titration curve of the monomeric MAA at $c_m = 100$ mM (10^{-2} g/g). In (b), the theoretical results are plotted for the same polymer concentrations: $c_m = 1$ mM (dotted curve); $c_m = 10$ mM (short dashes); $c_m = 100$ mM (long dashes). The solid line corresponds to the mean-field solution (no correlations and no connectivity) for $c_m = 100$ mM. It reproduces nicely the conventional monomeric titration curve. The polymer parameters we take are: $a = 5$ Å, $f = 1/3$, and $pK_a = 4.5$.

mesophase separation and becomes spatially modulated. If, however, the instability is at $q = 0$, the system undergoes a macrophase separation. In our case this occurs when

$$v c_m = w c_m^2 + \frac{1}{N} + \frac{f^2 A^2 c_m}{c_{eff}} \tag{38}$$

Recall that c_{eff} and A depend on the pH and the degree of neutralization.

III. Experiment

A. Preparation of Samples. The copolymer polyelectrolyte chains used in this study are prepared by standard emulsion polymerization techniques using neutral ethyl acrylate (EA) monomers and methacrylic acid (MAA) monomers. The methacrylic acid is a weak acid with $pK_a = 4.5$. The weight fraction of MAA in the copolymer is equal to 0.35, taken to be $f = 1/3$ in the theoretical section. The emulsion polymerization is performed under starved monomer conditions. Under these conditions, the MAA and EA monomers are evenly distributed along the polymer chain. From size-exclusion chromatography, we have estimated the molecular weight of the chains to be of the order of 10^6 daltons, corresponding to a polymerization index of $N \simeq 10^4$. Because neutral MAA-EA copolymers are insoluble in water, a suspension of latex particles, each consisting of many MAA-EA chains, is obtained at the end of the synthesis. The precipitate is carefully washed by ultrafiltration to remove surfactants, unreacted monomers, and initiators. This cleaning procedure is stopped when the resistivity of the water flushed through the separation membrane is that of pure water (18.2 MΩ/m). The solid content of the stock solution is then determined accurately by drying and weighing.

B. Titration Measurement. Polymer solutions at different weight concentrations are prepared by mixing weighted amounts of the stock solutions with deionized water. The solution is carefully degassed with nitrogen to prevent dissolution of CO_2. Each of the polyelectrolyte solutions is neutralized by a NaOH solution with a molar concentration ranging from 0.1 to 2 M depending on the polymer concentration. Upon neutralization, the methacrylic acid is neutralized and repulsive forces due to the negative charges cause the chain to expand, resulting in the progressive solubilization of the polymer chains. As a result, the solution becomes transparent and its viscosity increases. In the following, we shall characterize the neutralization of the polymer chains by the degree of neutralization, $\gamma = c_B/(f c_m)$, which is the ratio of the added base to the available acids groups. Titration experiments are performed using a pH meter (Metrohm 691) with a combined glass electrode. The measurements are made at 20 °C with constant stirring under a nitrogen atmosphere. In parallel, the conductivity of the solution is measured (Metrohm 712).

The measurements reveal that all small ions present in solution are free and contribute to the conductivity. This was checked at different γ values by changing the polymer concentration. The measured conductivity is the exact sum of the conductivities coming from the Na^+ ions (whose concentration is known from the amount of added NaOH base) and the H^+, and OH^- ions (known from the pH), whereas the small contribution of the polymer is negligible. These conductivity measurements demonstrate that the distribution of small ions is homogeneous in the solution, and no evidence for the Donnan effect and counterion condensation is observed.

IV. Results: Comparison of Experiments with Theory

In this section we present the experimental results for the titration curves of MAA-EA copolymers and compare them with the theory of section II. Figure 1(a) shows the titration curves measured for different polymer concentrations. They differ substantially from the titration curves of monomeric methacrylic acid (MAA). Methacrylic acid in aqueous solution has the typical behavior of a weak monomeric acid. The pH increases monotonically with γ, takes the value $pK_a = 4.5$ for $\gamma = 0.5$, and then jumps near $\gamma = 1$. By contrast, the titration curves of MAA-EA copolymers exhibit the following behavior: in the range $0 \lesssim \gamma \lesssim 0.2$, the pH increases sharply to a plateau value which remains nearly constant up to $\gamma \approx 1$, where the amount

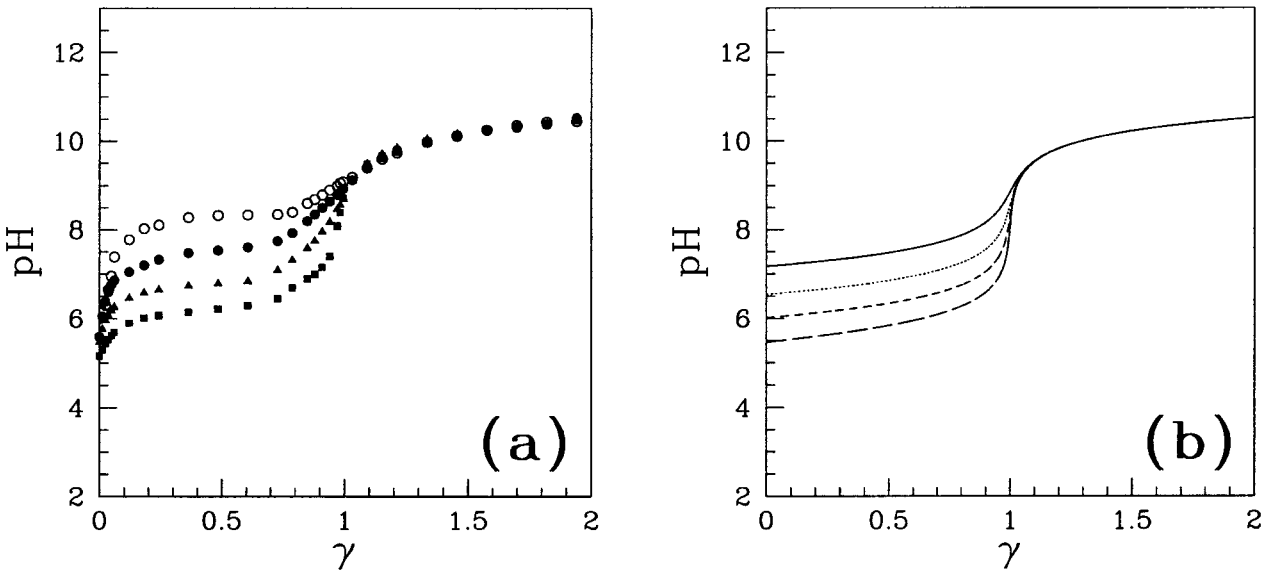

Figure 2. pH plotted as a function of the degree of neutralization, γ, for different amounts of added salt. The experimental values in (a) are compared with the theoretical ones in (b). The polymer concentration is $c_m = 1$ mM (10^{-4} g/g). The concentration of NaCl in the solution is $c_{NaCl} = 0$ M (open circles/solid line), 1 mM (full circles/dotted curve), 10 mM (full diamonds/short dashes), and 100 mM (full squares/long dashes). The theoretical curves are calculated using the same parameters as in Figure 1.

of added base equals that of the monomer (neutralization point). The jump of the pH for $\gamma \lesssim 0.2$ is associated with a swelling phase transition of the latex particles, i.e., a change of conformation of the chains. A similar phenomenon has been observed during the titration of pure poly(methacrylic acid).[23]

Let us mention that it is possible to calculate the swelling transition of the polymer as a function of monomer concentration, c_m. This can be done by minimizing the free energy with respect to c_m (in addition to the other annealed degrees of freedom discussed above). Any nonconvexity of the free energy signals the existence of a polymer precipitate in excess water.

In Figure 1 several titration curves are plotted for different concentrations of the same MAA-EA copolymer. As the concentration c_m increases, the jump in the pH at $\gamma \approx 1$ increases. Note that the deviation between the pH of the MAA monomeric acid and the MAA-EA copolymers ($c_m = 100$ mM in Figure 1) is large in the plateau region ($\gamma < 1$). On the other hand, the deviation is quite small for $\gamma > 1$ when the acid is almost completely dissociated. The value of the pH at the plateau depends strongly on the polymer concentration: the larger the c_m, the lower the plateau. It is surprising that even though MAA-EA copolymers contain carboxylic groups, the plateau value of the pH below $\gamma = 1$ may be neutral or even greater than 7.

This difference in behavior between the MAA monomers and MAA-EA copolymers might be associated with a complex structure of the MAA-EA copolymer for $\gamma \lesssim 1$. Collapsed microdomains may exist on the chains because of the competition between the hydrophobic attraction and the Coulomb repulsion. The plateau region suggests the existence of such collapsed microdomains along the chains. For $\gamma \gtrsim 1$ the chains are in a swollen state, and their behavior resembles that of a monomeric weak acid.

In Figure 1(b) we plot for comparison the titration curves as calculated from the theory. The titration equations presented in section II.B are solved numerically by an iteration procedure, starting from the mean field values as the first iteration and including the corrections of the second iteration.

Because there are a couple of unknown physical parameters (such as the second and third virial coefficients, v, w, and the monomer size a), we do not try to fit the experimental titration curve. Rather, we note that the corresponding theoretical curves look very similar to the experimental ones, demonstrating the same type of plateau for low γ and the same trend with the monomer concentration.

Figure 2 shows the effect of adding a monovalent salt (NaCl). The overall shape of the titration curves remains unchanged. However, the value of the pH at the plateau decreased upon the addition of salt, whereas the pH for $\gamma \gtrsim 1$ is essentially not dependent of the salt concentration. This indicates that neutralization of the carboxylic groups carried by the chains becomes easier as the ionic strength is decreased. As the Coulomb interaction is screened by the salt, less correlation occurs between charged groups along the chain when their distance is larger than the Debye length. Therefore, monomers separated by distances larger than the Debye length can dissociate independently from each other. For $\gamma \gtrsim 1$, almost all the charged groups on the chains are dissociated; thus, the salt has no effect on the pH. The comparison between experiment and theory is presented in parts (a) and (b), where a good agreement can be observed. Note the larger deviation from the experimental results for zero salt concentration.

In Figure 3, the plateau value of the pH is plotted on a semilog plot as function of the ionic strength $c_I = c_{Na} + c_H + c_{Cl} + c_{OH}$. The plateau value of the pH is taken at $\gamma = 0.5$. It is interesting to note that the different points taken at various salt and base concentrations collapse on a single curve. This result indicates that the pH is dominated by electrostatic effects and not by conformation changes of the chains. When the ionic strength increases, the fixed charges carried by the polymer are screened and the energy associated with the dissociation of a carboxylic group decreases.

This behavior can be characterized semiquantitatively by noting that when $\gamma \simeq 1/2$, the pH is much higher than the pK_a. The mean field γ obtained from F_0 is $\gamma = A + (c_{OH} - c_H)/(fc_m) \to 1$, whereas the correction to γ (beyond mean field) is close to 1/2. To first order in $10^{pK_a - pH}$ the plateau value can be obtained from the simplified free energy, section II.A.3, and reads

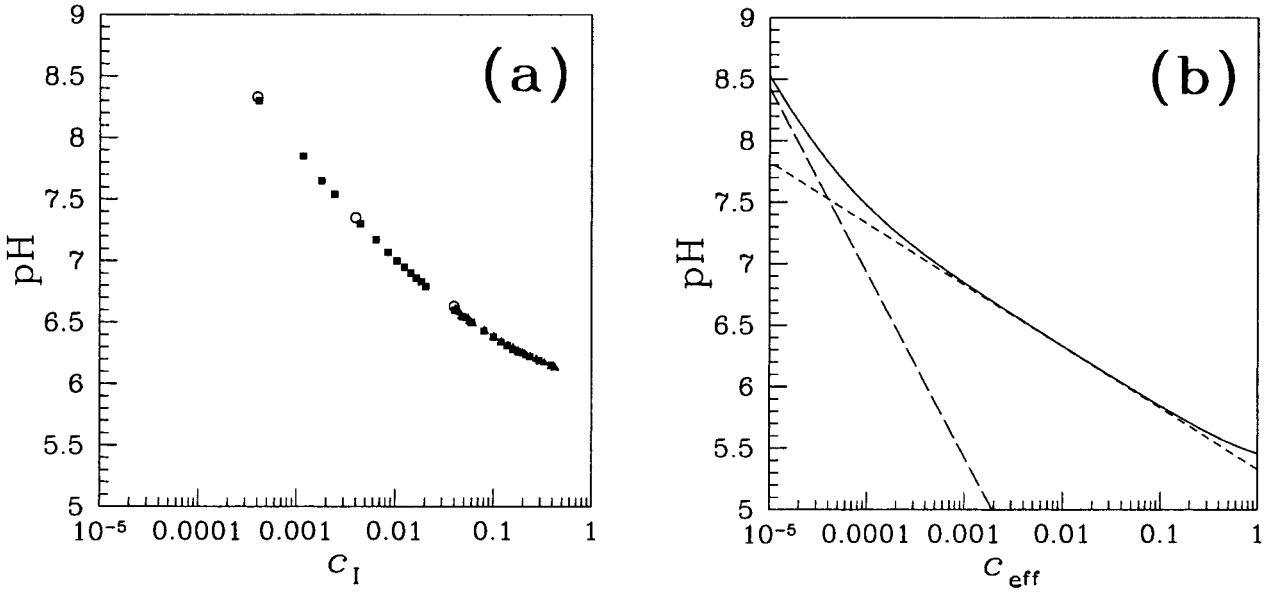

Figure 3. Semilog plot of the pH at the plateau as a function of the ionic strength. Comparison between experimental results (a) and theoretical calculation (b). The experimental measurements are plotted in (a) as function of the total amount of small ions, c_I. The open circles give the pH of salt-free solutions at different monomer concentrations extracted from Figure 1. The full symbols give the pH of solutions with increasing amounts of added salt: $c_m = 1$ mM (10^{-4} g/g), full circles; and $c_m = 100$ mM (10^{-2} g/g), full triangles. The data collapse indicates that the pH depends only on the total ionic strength. The theoretical results are plotted in (b) as a function of $c_{eff} = c_I + fA(1 - A)c_m$ using the same parameters as in Figure 1. See text for details of the approximations made in the calculation. The long and short dashed lines in (b) with slopes −3/2 and −1/2, respectively, are explained in the text.

$$\mathrm{pH}_{\mathrm{plateau}} \simeq \mathrm{p}K_a + \log_{10}\left[\kappa l_B + 24\pi f^2 c_m \frac{l_B^2 \kappa^{-3}}{a^2} + 24 f \frac{l_B \kappa^{-1}}{a^2}\right] \tag{39}$$

Recall that κ depends on the total concentration of ions in the system through eq 9. The above expression is used for the plot of the solid curve of Figure 3b, where the pH of the plateau is shown as a function of the effective ionic strength c_{eff} defined in eq 9. In this regime, the difference between c_{eff} and c_I is a small correction of the order $10^{\mathrm{p}K_a - \mathrm{pH}}$.

Equation 39 exhibits three different regimes depending on the relative importance of the various contributions to the logarithmic term. In each regime, c_H has a different power-law dependence on the total ionic strength $c_{eff} = c_I + fA(1 - A)c_m$, leading to different slopes in Figure 3. At low ionic strength, the second term dominates and $c_H \propto c_{eff}^{3/2}$ (long dashed line in Figure 3b). At intermediate ionic strength, the last term dominates and $c_H \propto c_{eff}^{1/2}$ (short dashed line). Finally, at high ionic strength (beyond the experimentally accessible values), $c_H \propto c_{eff}^{-1/2}$.

In Figure 4 the effect of polymer concentration and ionic strength on $S(q)$ is shown. The structure function is calculated at the plateau regime where $A \simeq 1$. The dependence on the controlled system parameters (the pH; the salt concentration; and the degree of neutralization, γ) is taken implicitly into account in c_{eff}. At low values of c_{eff}, the structure function exhibits a peak at finite q corresponding to the most favorable density−density fluctuations. As c_{eff} increases, $S(q \to 0)$ increases until the peak at $q > 0$ disappears. This increase is accompanied by an increase in the osmotic compressibility of the solution.

The effect of varying the polymer concentration c_m at a fixed c_{eff} is depicted in the inset. The peak is stronger at lower polymer concentrations, indicating that fluctuations become considerably stronger at lower concentrations. This effect agrees well with the titration curves shown in Figure 1. Indeed, at low polymer concentrations the shift in the titration curve is stronger than at high concentrations. The peak position shifts to higher wavenumbers (smaller length scale) at higher concentrations, similar to the correlation length of polymer solutions that decreases with increasing polymer concentration. A similar behavior has been observed in scattering experiments performed on a polybase derivative of poly(thioether).[24]

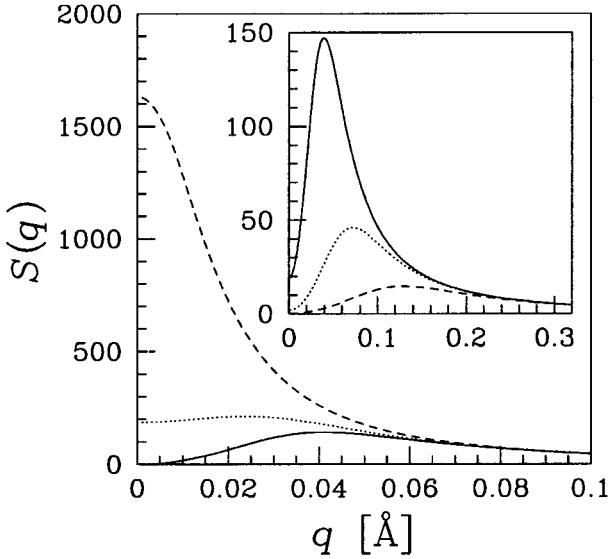

Figure 4. The structure function, $S(q)$, as function of the wavenumber q. The structure function is calculated at the plateau of the titration curve where $A \simeq 1$. The physical parameters used in the calculation are $a = 5$ Å, $v = 25$ Å^3, $w = 100$ Å^6, $N = 10^4$, $f = 1/3$ and $\mathrm{p}K_a = 4.5$. The monomer concentration is $c_m = 1$ mM, and the effective ionic strength is $c_{eff} = 0.01$ mM (solid line), $c_{eff} = 10$ mM (dotted curve), and $c_{eff} = 100$ mM (dashed curve). In the inset, the effective ionic strength is fixed at $c_{eff} = 1$ mM, whereas the polymer concentration is varied: $c_m = 1$ mM (solid line), $c_m = 10$ mM (dotted curve), and $c_m = 100$ mM (dashed curve).

V. Conclusions

We have presented an experimental study of the titration of weak polyacids by a strong base. Our experimental findings,

performed on solutions of MAA-EA copolymers, are supported by theoretical calculations, which show similar trends of the pH variation with the concentration of added base, salt, and polyacid.

Titration experiments are among the simplest and most useful experimental tools for probing the degree of neutralization of monomeric and polymeric acids. Because titration curves of weak acids are universal, any deviation from this behavior, as observed here, can be the signature of a complex behavior coupling Coulombic and hydrophobic interactions.

The most striking feature is the existence of a plateau in the pH for low degrees of neutralization. The plateau in the pH is at a higher value than the corresponding pH of the monomeric acid, indicating that the charges on the chain inhibit the dissociation of other charged groups. The pH is not affected strongly by further addition of the base up to the neutralization point, $\gamma = 1$. This probably is due to the existence of collapsed microdomains along the chains for $\gamma \lesssim 1$. The pH at the plateau decreases as function of the ionic strength. This demonstrates that nonspecific electrostatic interactions are responsible for the existence of the plateau, because the pH depends mostly on the concentration of small ions and not on their type (for a fixed degree of neutralization).

The theory presented above includes one-loop corrections to the mean-field free energy. On the mean-field level, no difference exists between the polymeric and monomeric titration curves except for the translational entropy of the chains. The one-loop correction couples the chain connectivity with the electrostatics and induces the large deviations in the titration curves. We modeled the polyacid as flexible chains using the standard Debye function.

Even though the one-loop expansion treats the concentration fluctuations better, its domain of validity is that of the random phase approximation (RPA), namely semidilute or concentrated solutions of polyelectrolytes. This is the case in the experiments reported here.

Our formalism can also be applied to different models of chain elasticity. In particular, for the case of semiflexible chains, the same titration equations are obtained with a modified Debye function, taking into account the persistence length of the chains.

Finally, it will be interesting to complement this study with scattering experiments, in which it might be possible to resolve the chain microstructures and relate them to the degree of ionization of the chains.

Acknowledgment. We thank Y. Burak for discussions and a critical reading of the manuscript. I.B. gratefully acknowledges the support of the Chateaubriand postdoctoral fellowship and the hospitality of the ATOFINA research center at Levallois-Perret. D.A. acknowledges partial support from the U.S.−Israel Binational Foundation (BSF) under Grant 98-00429, and the Israel Science Foundation, founded by the Israel Academy of Sciences and Humanities−Centers of Excellence Program.

References and Notes

(1) Oosawa, F. *Polyelectrolytes*; Marcel Dekker: New York, 1971.

(2) De Gennes, P. G. *Scaling Concepts in Polymer Physics*; Cornell University: Ithaca, NY, 1979.

(3) Barrat, J. L.; Joanny, J. F. *Adv. Chem. Phys.* **1996**, *94*, 1.

(4) Tanaka, T. *Phys. Rev. Lett.* **1978**, *40*, 820.

(5) Philippova, O. E.; Hourdet, D.; Audebert, R.; Khokhlov, A. R. *Macromolecules* **1997**, *30*, 8278.

(6) Joanny, J. F.; Leibler, L. *J. Phys. (Paris)* **1990**, *51*, 547.

(7) Kokufuta, E.; Wang, B.; Yoshida, R.; Khokhlov, A. R.; Hirata, M. *Macromolecules* **1998**, *31*, 6878.

(8) Raphael, E.; Joanny, J. F. *Europhys. Lett.* **1990**, *13*, 623. Wittmer, J. P. Ph.D Thesis, Université L. Pasteur, Strasbourg, France, 1994 (unpublished).

(9) Hasa, J.; Ilavský, M. *J. Polym. Sci.* **1975**, *13*, 263.

(10) Tirtaatmadja, V.; Tam, K. C.; Jenkins, R. D. *Macromolecules* **1997**, 30, 3271.

(11) Tam, K. C.; Farmer, M. L.; Jenkins, R. D.; Bassett, D. R. *J. Polym., Sci., Part B: Polym. Phys.* **1998**, *36*, 2275.

(12) Katchalsky A.; Michaeli, I. *J. Polym. Sci.* **1955**, *15*, 69.

(13) Hasa, J.; Ilavský, M.; Dušek, K. *J. Polym. Sci.* **1975**, *13*, 253.

(14) Brereton, M. G.; Vilgis, T. A. *Macromolecules* **1990**, *23*, 2044. Vilgis, T. A.; Borsali, R. *Phys. Rev. A.* **1991**, *43*, 6857. Brereton, M. G.; Vilgis, T. A. *J. Phys. I (Paris)* **1992**, *2*, 581.

(15) Napper, D. H. *Polymer Stabilization of Colloidal Dispersions*; Academic Press: London, 1993.

(16) Jenkins, R. D.; Lelong, L. M.; Bassett, D. R. In *Hydrophilic Polymers: Performance with Environmental Acceptability*; Glass, J. E., Ed.; ACS Symposium Series 248; American Chemical Society, Washington, DC, 1996, p 425.

(17) Atkins, P. W. *Physical Chemistry*; Oxford University: Oxford, U.K., 1985.

(18) Mandel, M. In *Encyclopedia of Polymer Science and Engineering*, 2nd ed.; Mark, H. F., Bikales, N., Overberger, C. G., Menges, G., Kroschwitz, J. I., Eds.; J. Wiley: New York, 1988; Vol. 11, p 739.

(19) Strauss, U. P.; Schlesinger, M. S. *J. Phys. Chem.* **1978**, *82*, 571.

(20) For more details on volume and conformational transitions, see, e.g., Shibayama, M.; Tanaka T. *Adv. Polym. Sci.* **1993**, *109*, 1. Khokhlov, A. R.; Starodubtzev, S. G.; Vasilevskaya, V. V. *Adv. Polym Sci.* **1993**, *109*, 123.

(21) Borrega, R. Ph.D. Thesis, Université de Paris VI, France, 1999 (unpublished).

(22) Borukhov, I.; Andelman, D.; Orland, H. *Eur. Phys. J. B* **1998**, *5*, 869.

(23) Heitz, C.; Raviso, M.; François, J. *Polymer* **1999**, *40*, 1637.

(24) Auvray, X.; Anthore, R.; Petitpas, C.; Huguet, J.; Vert, M. *J. Phys. (Paris)* **1986**, *47*, 893.